Electronic Supplementary Information

Accurate determination of enantiomeric excess of an amino acid using an extended-gate-type organic transistor

Yijing Zhang,[a] Yui Sasaki,[a,b,c] Xiaojun Lyu,[a] Jun-ichi Ogawa,[d] Hidenosuke Itoh[d] and Tsuyoshi Minami*[a]

[a] Institute of Industrial Science, The University of Tokyo, 4-6-1 Komaba, Meguro-ku, Tokyo, 153-8505, Japan

Corresponding author: tminami@g.ecc.u-tokyo.ac.jp

[b] Research Center for Advanced Science and Technology, The University of Tokyo, 4-6-1, Komaba, Meguro-ku, Tokyo, 153-8904 Japan

[c] JST PRESTO, 4-1-8 Honcho, Kawaguchi, Saitama, 332-0012, Japan

[d] Yokogawa Electric Corporation, 2-9-32 Nakacho, Musashino, Tokyo 180-0006

Contents

1. Regents and materials **S2**
2. DFT Calculations for the optimization of the pre-organized structure **S2**
3. Optimization of a molar ratio for MIP fabrication **S2**
4. Fabrication and characterization of the MIP electrode **S4**
5. Fabrication and characterization of the OFET device **S6**
6. Selected transistor characteristics in chemical sensing **S7**
7. %ee Determination **S8**
References

1. Regents and materials

Commercially available reagents and materials were used in device fabrication and analyte detection without further purification or pre-treatment.

For fabrication of the OFET device: A glass wafer (model: Eagle XG, 2 cm × 2.5 cm) utilized as a substrate was obtained from Corning, Inc. A gate electrode was fabricated using aluminum (Al) wire (1ϕ) purchased from Furuuchi Chemical Co., Ltd. Tetradecylphosphonic acid (TDPA, from Tokyo Chemical Industry Co., Ltd.) and 2-propanol (from Kanto Chemical Co., Inc.) were employed to form a monolayer-based dielectric. Au particles for source and drain electrode fabrication were purchased from Tanaka Kikinzoku Kogyo Co., Ltd. An organic semiconductor material, poly{2,5-bis(3-tetradecylthiophen-2-yl)thieno[3,2-*b*]thiophene} (PBTTT-C14) and 1,2-dichlorobenzene were purchased from Merck KGaA. An amorphous fluoropolymer (CYTOP™, model: CTL-809M) was supplied from AGC Co., Ltd.

For fabrication of the extended-gate MIP electrode: A substrate made of polyethylene naphthalate (PEN) film was supplied from TOYOBO Co., Ltd. Hydrogen tetrachloroaurate(III) tetrahydrate ($HAuCl_4$) for the formation of an Au nanostructure (AuNS) layer was obtained from FUJIFILM Wako Pure Chemical Industries, Ltd. A functional monomer (*i.e.*, 1,2-diaminobenezene) and a template (i.e., L-histidine) for the formation of an MIP layer were purchased from Tokyo Chemical Industry Co., Ltd. Sodium hydroxide (NaOH) for the extraction of the template was purchased from Kanto Chemical Co., Inc.

For electrical measurements and chemical sensing: A conductive silver paste (model: D-500) was purchased from FUJIFILM Wako Pure Chemical Industries, Ltd. An Ag/AgCl reference electrode and a Pt wire-based working electrode were obtained from BAS Inc. Amino acid families for the selectivity test, L-lysine, L-tyrosine, L-tryptophan, and L-phenylalanine were the product of Tokyo Chemical Industry Co., Ltd. D-Histidine, disodium hydrogenphosphate dodecahydrate, and sodium dihydrogenphosphate dihydrate were obtained from Kanto Chemical Co., Inc. All aqueous solutions used in this assay were prepared with Milli-Q water (18.2 MΩ·cm).

2. DFT Calculations for the optimization of the pre-organized structure

All calculations for the optimization of pre-organized structures for MIP were performed using the B3LYP-D3(BJ) function with the 6-311+G* through Gaussian 16 Revision C.01.18.[S1] The B3LYP function was appended with DFT-D3 correction using the Becke-Johnson damping function. The Basis Set Superposition Error (BSSE) energy was calculated at the same level of theory using the counterpoise (CP) correction method. In addition, the PCM solvent model (*i.e.*, water was used as a solvent) was employed for the calculation of the electronic energy of the complexes. Noncovalent interactions based on Hirshfeld partition of molecular density (IGMH) analysis for the optimized geometry structures were visualized by wave function analysis by Multiwfn[S2,3] and rendered by the Visual Molecular Dynamics (VMD) program.[S4] The initial geometries of the functional monomers were determined considering hydrogen bonds between the monomers and binding sites of histidine. As stoichiometry, two of the functional monomers were initially distributed near the carboxy group of the template. Next, the other two monomers were distributed near binding sites (i.e., the primary amino group and aromatic amino moiety).

3. Optimization of a molar ratio for MIP fabrication

The appropriate molar ratio between the monomer and the template was determined by both DFT calculations and experimental investigations. In this demonstration, the binding energies of the pre-organized complexes at 3:1, 4:1, and 5:1 molar ratios (= 1,2-diaminobenzene: L-His) were estimated in Table S1. The DFT calculation results revealed insufficient interactions between the monomer and the template at 3:1. Meanwhile, although a slightly more stable complex was observed at the 5:1 molar ratio, the surplus monomer (dark gray-highlighted) did not contribute to interactions with the template. Thus, the significant change in binding energy between 4:1 and 5:1 is not observed in comparison to that between 3:1 and 4:1. Indeed, the low contributed monomer caused a decrease in the cavity density inside the MIP, which reflected the lower response of the MIP electrode (at 5:1) to L-His than 4:1 in the electrochemical measurement (Fig. S3).

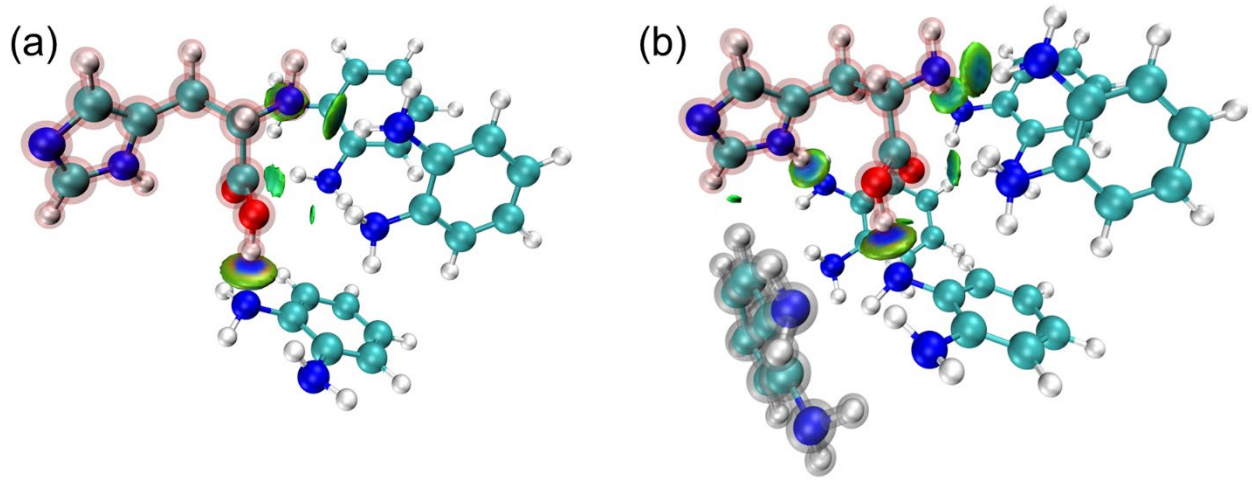

Fig. S1 The isosurface IGM figure of the optimized complexes of 1,2-diaminobenzene and L-histidine at (a) 3:1 and (b) 5:1 molar ratios. The blueish-green ellipsoid areas indicate non-covalent interactions.

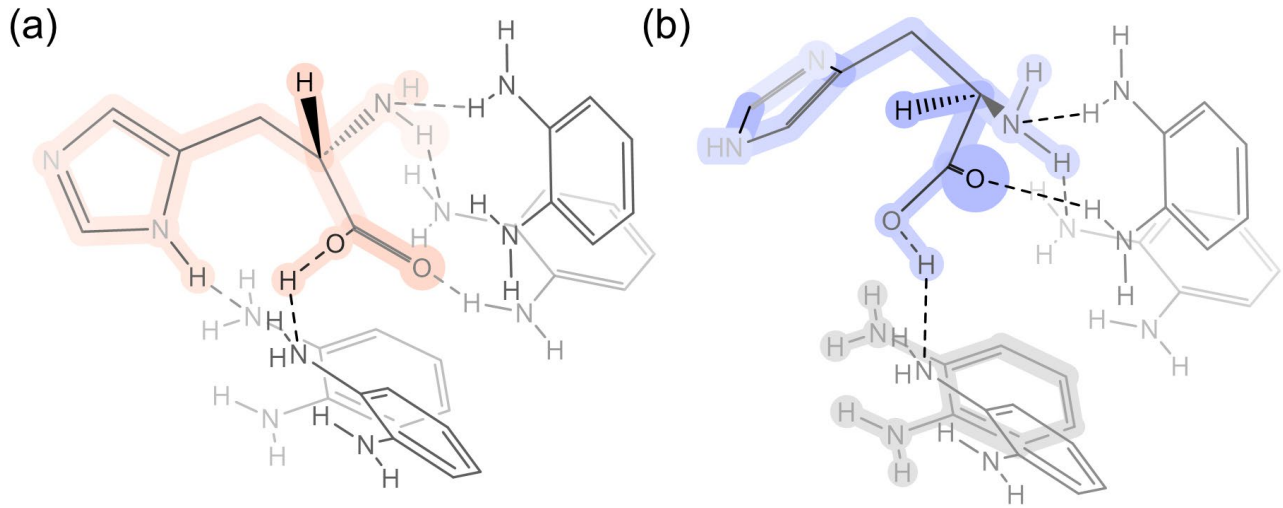

Fig. S2 Chemical structures of pre-organized complexes between 1,2-diaminobenzene and (a) L-His and (b) D-His. The gray-highlighted monomer did not contribute to non-covalent interactions with D-His.

Table S1 Calculated binding energy at different ratios of 1,2-diaminobenzene and L-histidine (kJ/mol)

Monomer Quantity	3:1	4:1	5:1
Binding Energy [a] (BSSE [b] Corrected)	−128.9	−155.6	−166.2

[a] Binding Energy = *E*(complex) − *E*(monomers) − *E*(templates)

[b] Basis Set Superposition Error (BSSE)

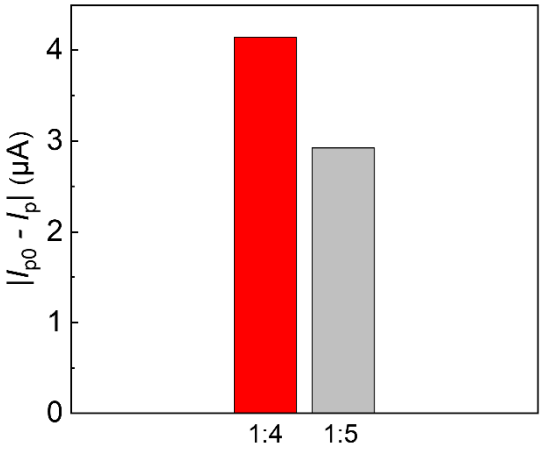

Fig. S3 Comparison of DPV current responses of 1:4 (red) and 1:5 (gray) (= template : monomer) electrodes against L-histidine (10 mM). The terms I_{p0} and I_p mean the peak currents before and after adding L-histidine.

4. Fabrication and characterization of the MIP electrode

A MIP-functionalized Au electrode was fabricated through a sequential process. First, a gold layer (100 nm) was thermally deposited onto a PEN film using an evaporation instrument (SVC-700TMSG/SVC-7PS80, SANYU Electron). Next, AuNS was formed on the thermally deposited Au electrode surface *via* chronoamperometry in a $HAuCl_4$ solution (100 mM) at −0.1 V for 60 s. Subsequently, a polymer layer was electrochemically deposited by performing cyclic voltammetry (CV) with 20 cycles in a phosphate buffer solution (100 mM) at pH 6.0 containing 1,2-diaminobenzene (8.0 mM) and L-histidine (2.0 mM). Non-imprinted polymer (NIP) was formed without using the template. The CV polymerization was carried out at a scan rate range of 20 to 50 mV/s over a potential window of 0 to 0.8 V. The template was removed from the polymer layer by applying three additional CV cycles at the potential range of −0.8 to 0.8 V at a scan rate of 20 mV/s in a NaOH solution (100 mM). All electrochemical deposition and template extraction processes were carried out using a three-electrode system (SP-300 potentiostat, Biologic).

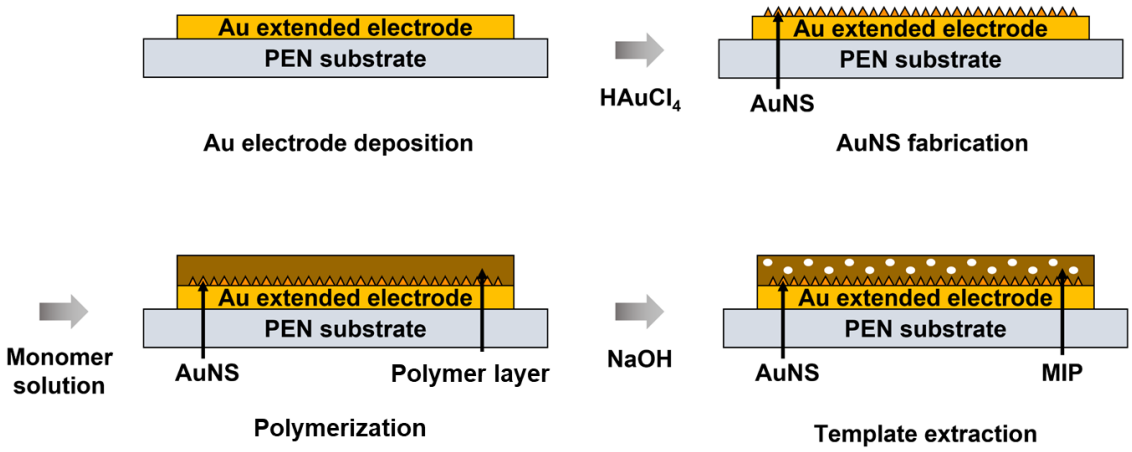

Fig. S4 Schematic illustration of the fabrication procedure for an Au MIP electrode.

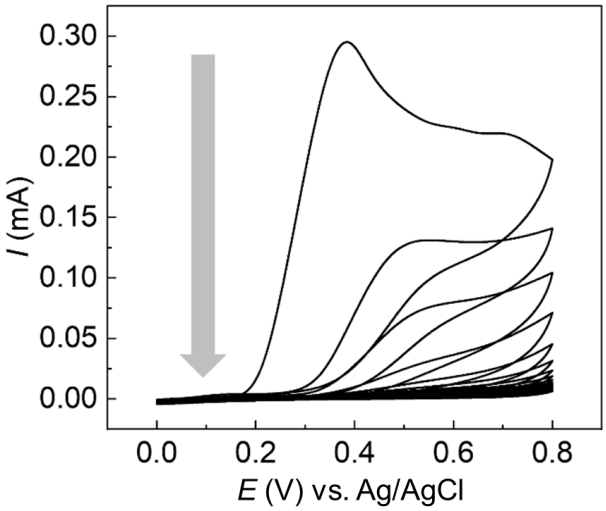

Fig. S5 Cyclic voltammograms recorded during the electrochemical polymerization with 20 cycles in a phosphate buffer solution (100 mM) at pH 6.0 at 25 °C containing 1,2-diaminobenzene (8.0 mM) and L-histidine (2.0 mM).

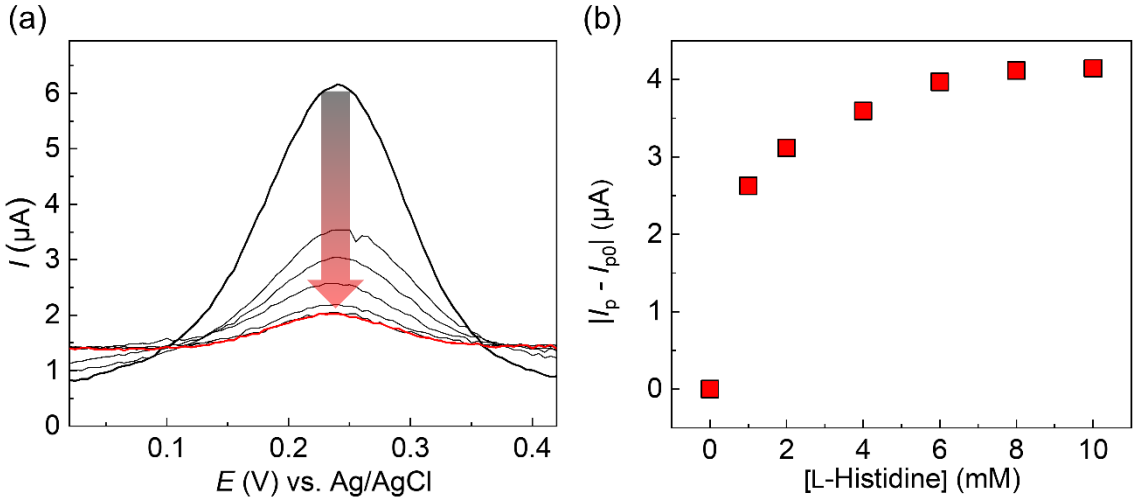

Fig. S6 (a) DPV responses and (b) titration isotherm of the MIP-functionalized electrode upon adding L-histidine (0.0–10 mM) in a phosphate buffer solution (100 mM) at pH 6.0 at 25 °C containing $K_3Fe(CN)_6$ (5.0 mM) and KCl (100 mM). The terms I_{p0} and I_p mean the peak currents before and after adding L-histidine.

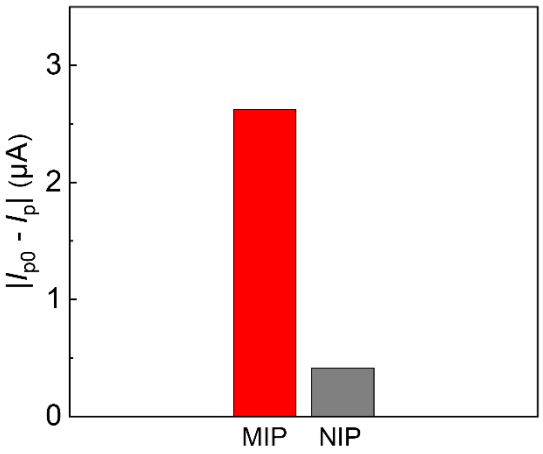

Fig. S7 Comparison of DPV current responses of MIP (red) and NIP (gray) electrodes against L-histidine (1.0 mM). The terms I_{p0} and I_p mean the peak currents before and after adding L-histidine.

5. Fabrication and characterization of the OFET device

An organic field-effect transistor (OFET) device was fabricated following the procedure. First, a glass substrate was cleaned thoroughly using a piranha solution (H_2SO_4:H_2O_2 = 4:1, v/v) to remove organic contaminants. Subsequently, an aluminum (Al) gate electrode was vacuum-deposited onto the substrate through a patterned metal mask using thermal evaporation equipment (SVC-700TMSG/SVC-7PS80, SANYU Electron). An aluminum oxide (AlO_x) dielectric layer was formed by reactive ion etching (RIE) (SAMCO RIE-10NR). A CYTOP™ (CTX-809M) solution was then spin-coated onto the dielectric layer (SPINCOATER 1H-D7, MIKASA), followed by baking at 110 °C for 10 minutes in an inert atmosphere glove box (UL-1300A-MSP, UNICO), and subsequently patterned again *via* RIE to form a bank structure. A self-assembled dielectric layer was prepared by immersing the device into a 2-propanol solution containing TDPA (10 mM) for 15 hours under ambient conditions. After immersion, the device was rinsed with 2-propanol, dried using nitrogen gas, and then baked at 110 °C for 30 minutes in the inert atmosphere glove box. Source and drain electrodes made of Au were then deposited through a patterned shadow mask. The organic semiconductor material (PBTTT-C14) dissolved in 1,2-dichlorobenzene (0.0075wt%) was drop-cast onto the channel region (width: 50 µm, length: 1000 µm). The semiconductor layer was annealed at 160 °C for 10 minutes in the inert atmosphere glove box. Finally, CYTOP™ was spin-coated as a passivation layer, followed by baking at 110 °C for 10 minutes under the same inert conditions. The characteristics of the manufactured OFET device were evaluated using a semiconductor parameter analyzer 4156B, Agilent. The transfer characteristics (Fig. S9(a)) were obtained by scanning gate voltages (V_{GS} = 0.5 to −3 V) at a certain drain-source voltage (V_{DS} = −2 V). The output characteristics (Fig. S9(b)) were measured at V_{DS} = 0 to −3 V at each V_{GS} condition (V_{GS} = 0 to −3 V, step: −1 V).

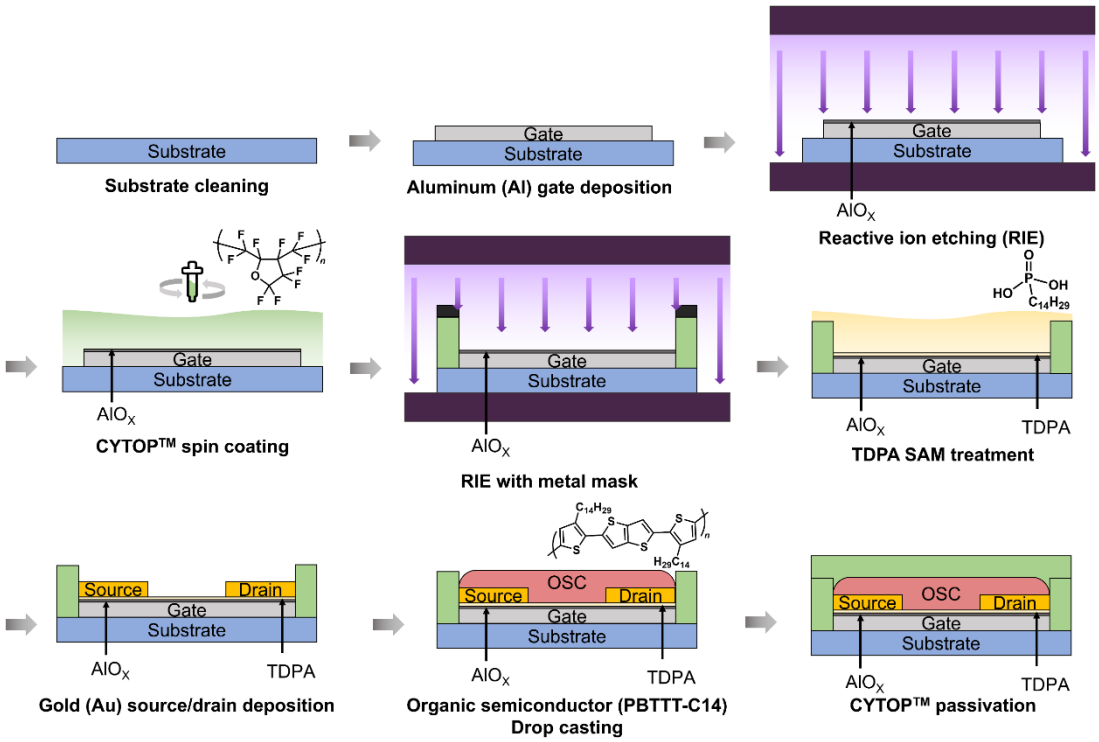

Fig. S8 Schematic illustration of the fabrication procedure for the OFET device.

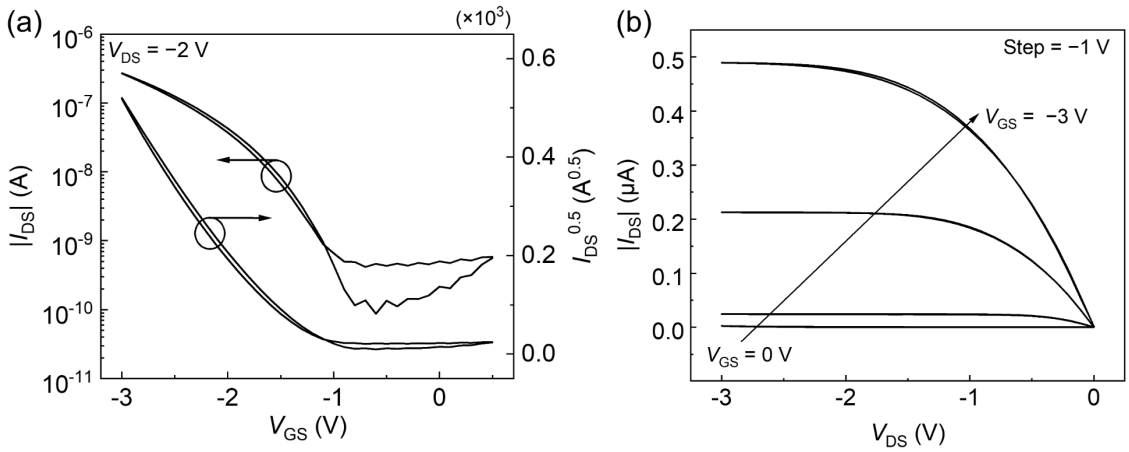

Fig. S9 (a) Transfer and (b) output characteristics of the fabricated OFET device under ambient conditions.

6. Selected transistor characteristics in chemical sensing

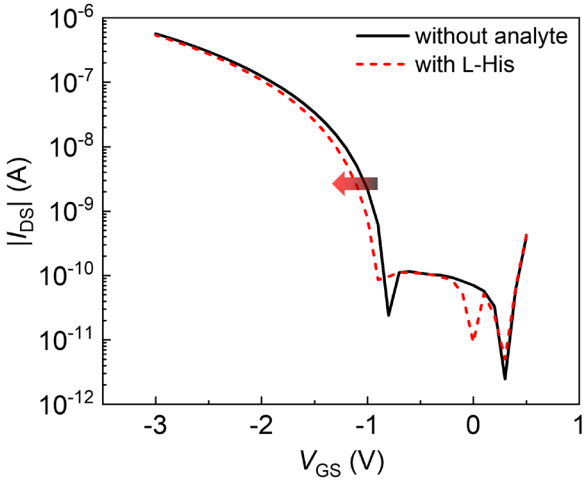

Fig. S10 Transfer characteristics of the MIP-OFET before (black line) and after adding L-histidine (L-His) (1.0 mM) (red dashed line) in a phosphate buffer solution (100 mM) at pH 6.0 at 25 °C.

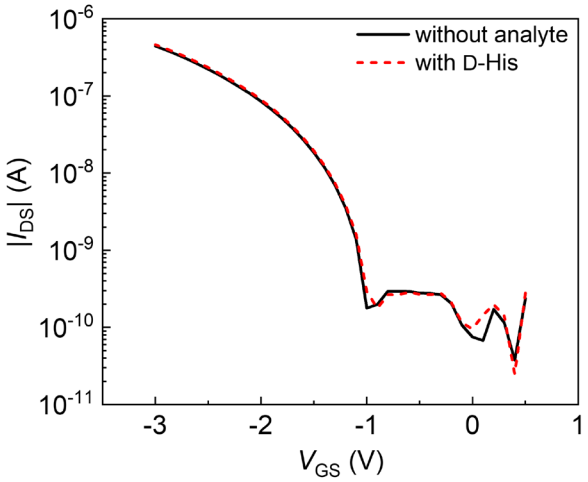

Fig. S11 Transfer characteristics of the MIP-OFET before (black line) and after adding D-histidine (D-His) (1.0 mM) (red dashed line) in a phosphate buffer solution (100 mM) at pH 6.0 at 25 °C.

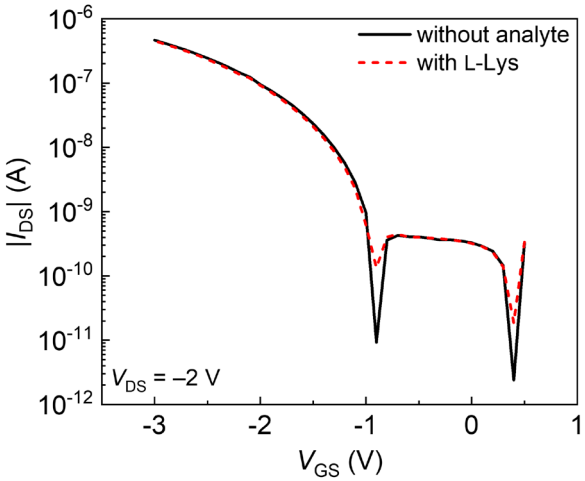

Fig. S12 Transfer characteristics of the MIP-OFET before (black solid line) and after adding L-lysine (L-Lys) (1.0 mM) (red dashed line) in a phosphate buffer solution (100 mM) at pH 6.0 at 25 °C.

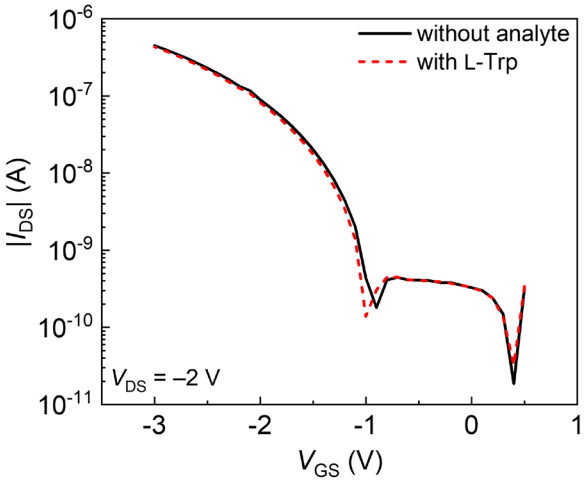

Fig. S13 Transfer characteristics of the MIP-OFET before (black solid line) and after adding L-tryptophan (L-Trp) (1.0 mM) (red dashed line) in a phosphate buffer solution (100 mM) at pH 6.0 at 25 °C.

Table S2 Calculated binding energy of the complexes of 1,2-diaminobenzene and an L-type aromatic amino acid at a 4:1 molar ratio (kJ/mol)

Template	L-Tyrosine	L-Phenylalanine	L-Tryptophan
Binding Energy [a] (BSSE [b] Corrected)	−46.5	−84.0	−72.0

[a] Binding Energy = *E*(complex) − *E*(monomers) − *E*(templates)

[b] Basis Set Superposition Error (BSSE)

7. %ee Determination

HPLC analysis: The HPLC analysis for the determination of enantiomeric purities of L- and D-His was carried out using LC-2010CHT (SHIMADZU). The system was equipped with a pump, a column oven, a UV absorption detector (200 nm), and a controller. A chiral column (DAICEL CROWNPAK® CR-1(+), 3.0 mm×150 mm×5 μm) was used for this analysis. A mixture of perchloric acid (pH 1.0) and acetonitrile (90:10, v/v) was used as the mobile phase. Each solvent was obtained from Kanto Chemical Co., Inc. The measurement conditions were as follows: flow rate at 0.1 mL/min; column temperature at 25 °C; injection volume was 5 μL.

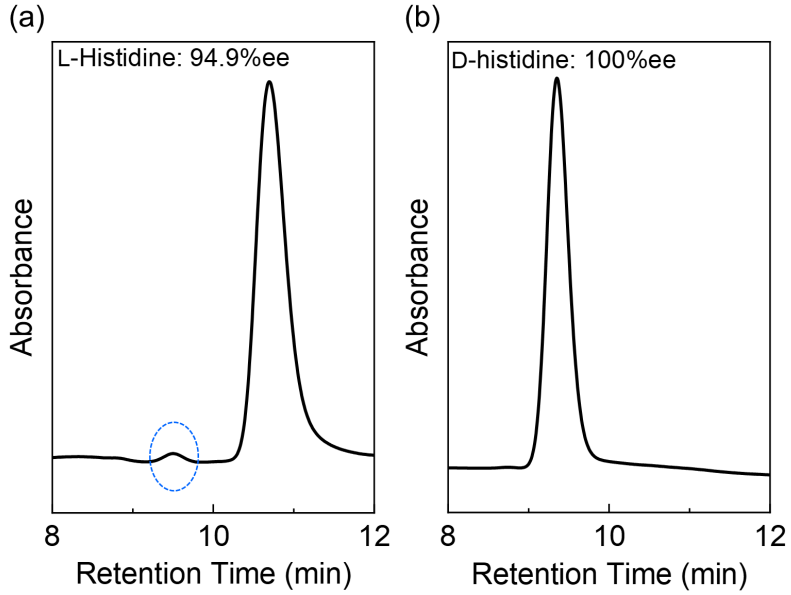

Fig. S14 HPLC charts of (a) L- and (b) D-histidine. A blue circle indicates a peak originating from D-histidine.

%ee determination using the MIP-OFET sensor: The stock solutions of L- and D-histidine were prepared in a phosphate buffer solution (100 mM, at pH 6.0 at 25 °C) with a total histidine concentration of 300 µM. The final concentration of histidine was adjusted to various %ee (from –5.1% to 87.9%, respectively). A semiconductor parameter analyzer (4156B, Agilent) was used to record the transfer characteristics depending on the different %ee values. The transfer characteristics at a range of V_{GS} = −1 to −3 V (0.1 V intervals) with three repetitions) were used for the inset data. The collected transfer characteristics were used to establish the calibration model and to predict %ee values simultaneously. Regression analysis (ϵ-support vector regression) was performed for the %ee determination using Solo 9.5 (Eigenvector Research). No data preprocessing was applied before the regression analysis.

Table S3 Calibration dataset for %ee determination

L-His (µM)	D-His (µM)	%ee
142.4	157.7	-5.1
156.6	143.4	4.4
199.3	100.7	32.9
213.5	86.5	42.4
242.0	58.0	61.3
256.2	43.8	70.8
263.3	36.7	75.6
270.5	29.5	80.3
273.3	26.7	82.2
279.0	21.0	86.0
281.9	18.1	87.9

Table S4 Prediction dataset for %ee determination

Actual L-His (μM)	Actual D-His (μM)	Actual %ee	Predicted %ee
170.8	129.2	13.9	15.3±5.4
185.1	114.9	23.4	25.7±0.9
227.8	72.2	51.9	47.7±3.6
276.2	23.8	84.1	83.8±1.8

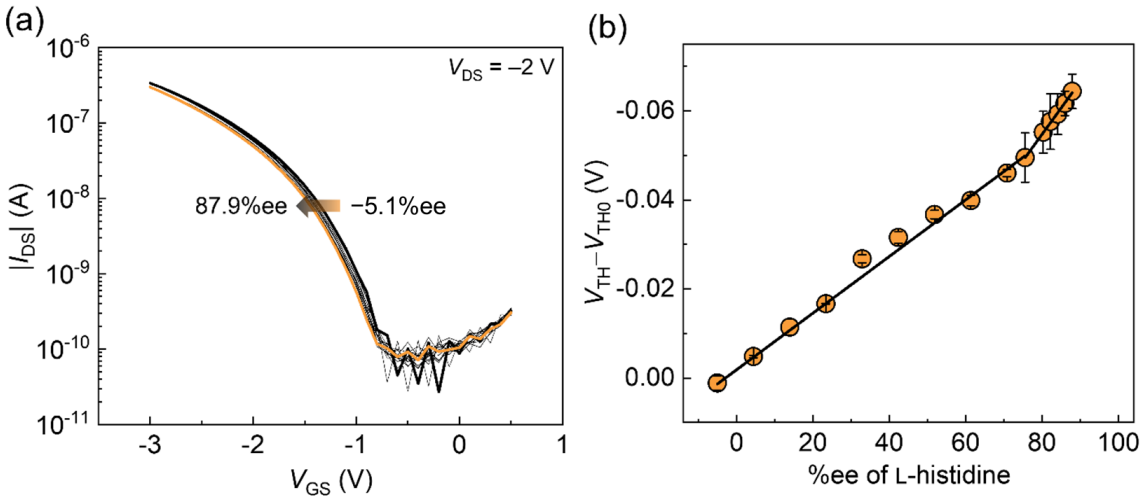

Fig. S15 (a) Transfer characteristics of the MIP-OFET in a phosphate buffer (100 mM) at pH 6.0 at 25 °C after adding different enantiomeric excesses of L-histidine (% ee values: −5.1%ee to 87.9%ee). The overall histidine concentration was set to 300 μM. The dataset was applied to the regression analysis using support vector machine (ϵ-support vector regression, Solo 9.5) for %ee determination. (b) Threshold voltage shifts of the MIP-OFET corresponding to %ee changes in L-His. The term V_{TH0} means threshold voltage at −5.1%ee.

References

S1. M. J. Frisch, G. W. Trucks, H. B. Schlegel, G. E. Scuseria, M. A. Robb, J. R. Cheeseman, G. Scalmani, V. Barone, G. A. Petersson, H. Nakatsuji, X. Li, M. Caricato, A. V. Marenich, J. Bloino, B. G. Janesko, R. Gomperts, B. Mennucci, H. P. Hratchian, J. V. Ortiz, A. F. Izmaylov, J. L. Sonnenberg, D. Williams-Young, F. Ding, F. Lipparini, F. Egidi, J. Goings, B. Peng, A. Petrone, T. Henderson, D. Ranasinghe, V. G. Zakrzewski, J. Gao, N. Rega, G. Zheng, W. Liang, M. Hada, M. Ehara, K. Toyota, R. Fukuda, J. Hasegawa, M. Ishida, T. Nakajima, Y. Honda, O. Kitao, H. Nakai, T. Vreven, K. Throssell, J. A. Montgomery Jr., J. E. Peralta, F. Ogliaro, M. J. Bearpark, J. J. Heyd, E. N. Brothers, K. N. Kudin, V. N. Staroverov, T. A. Keith, R. Kobayashi, J. Normand, K. Raghavachari, A. P. Rendell, J. C. Burant, S. S. Iyengar, J. Tomasi, M. Cossi, J. M. Millam, M. Klene, C. Adamo, R. Cammi, J. W. Ochterski, R. L. Martin, K. Morokuma, O. Farkas, J. B. Foresman and D. J. Fox, Gaussian 16 (Revision C.01), Gaussian, Inc., Wallingford CT, 2016.

S2. T. Lu and F. Chen, *J. Comput. Chem.*, 2012, **33**, 580–592.

S3. T. Lu and Q. Chen, *J. Comput. Chem.*, 2022, **43**, 539–555.

S4. W. Humphrey, A. Dalke and K. V. M. D. Schulten, *J. Mol. Graph.*, 1996, **14**, 33–38.